Materials Chemistry and Physics 228 (2019) 124–130

Contents lists available at ScienceDirect

Materials Chemistry and Physics

journal homepage: www.elsevier.com/locate/matchemphys

Increasing spontaneous wet adhesion of DOPA with gelation characterized by EPR spectroscopy

Yaman Göksel, Yasar Akdogan*

Materials Science and Engineering Department, İzmir Institute of Technology, İzmir, 35430, Turkey

HIGHLIGHTS

- Gelation of DOPA increases wet adhesion.
- Types of DOPA cross-linking mechanism affect the spontaneous adhesion.
- $(Cr_2O_7)^{2-}$ induced DOPA hydrogel adhere to SiO_2 and PS nanoparticles spontaneously.
- EPR spectroscopy provides the degree of surface coverage of nanoparticles.

GRAPHICAL ABSTRACT

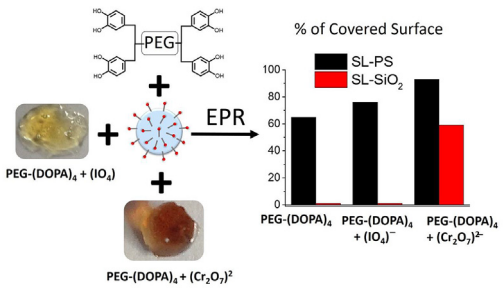

ARTICLE INFO

Keywords:
Wet adhesion
DOPA hydrogel
Surface coverage
EPR spectroscopy

ABSTRACT

The presence of water molecules around both adhesive materials and surface results in the hydration barriers that weaken adhesion. In nature, mussels attach to various types of surfaces by using 3,4-dihydroxyphenylalanine (DOPA) containing mussel foot proteins. DOPA shows wet adhesive properties before and after contribution in the hydrogel formation. Here, the wet adhesive properties of DOPA modified four armed poly (ethylene glycol) polymer (PEG-(DOPA)$_4$) and its hydrogels induced by $(IO_4)^-$ or $(Cr_2O_7)^{2-}$ ions are compared by using electron paramagnetic resonance (EPR) spectroscopy in terms of their surface coverages. In water, spin labeled hydrophobic polystyrene (SL-PS) and hydrophilic silica (SL-SiO_2) nanoparticles are prepared, and the percentages of their covered surface values are obtained. Without applying force, the adhesion to SL-PS increases in the order of PEG-(DOPA)$_4$ < PEG-(DOPA)$_4$ + $(IO_4)^-$ hydrogel < PEG-(DOPA)$_4$ + $(Cr_2O_7)^{2-}$ hydrogel with the percentages of surface coverages 65%, 76% and 93%, respectively. Although, neither of PEG-(DOPA)$_4$ polymer and $(IO_4)^-$ induced PEG-(DOPA)$_4$ hydrogel adhere to SL-SiO_2 nanoparticle spontaneously, $(Cr_2O_7)^{2-}$ induced PEG-(DOPA)$_4$ hydrogel adhere to SL-SiO_2 with a 59% of surface coverage. These results show that gelation mechanisms of DOPA have effect on the spontaneous adhesion of DOPA to the wet surfaces even for the hydrophilic silica surface.

1. Introduction

Marine mussels have inspired scientists to obtain adhesive materials that work underwater for a long time. It has been shown that 3,4-dihydroxyphenylalanine (DOPA) which is a posttranslationally modified tyrosine amino acid is responsible for both adhesive and cohesive properties of mussels [1]. Adhesive proteins of mussels known as mussel foot proteins (Mfps) contain DOPA up to 30 mol% [2]. During secretion of Mfps in water, DOPA plays a key role as a precursor of gelation of Mfps besides its adhesive function [3].

* Corresponding author.
E-mail address: yasarakdogan@iyte.edu.tr (Y. Akdogan).

https://doi.org/10.1016/j.matchemphys.2019.02.054
Received 8 November 2018; Received in revised form 30 January 2019; Accepted 17 February 2019
Available online 18 February 2019
0254-0584/

In the literature, DOPA and DOPA-like molecules have been attached to polymers in order to mimic adhesion ability of mussels [4–7]. Also, adhesive properties of them before and after cross-linking have been compared. Increasing the adhesive abilities of DOPA or DOPA-like molecules has been shown after gelation processes [7,8]. The most commonly used cross-linkers are oxidizing transition metals such as Fe^{3+} and $(Cr_2O_7)^{2-}$, and nonmetallic oxidants such as $(IO_4)^-$ and H_2O_2 [9]. Cross-linking mechanisms of DOPA in the presences of oxidizing agents are based on covalently bonding or coordinating coupling [10]. Even, in some cases gel is formed by dual cross-linking mechanisms depending on the oxidizing agents, pH and the ratio of DOPA:oxidizing agent [11].

In an aqueous media, hydration layers obstruct the formation of strong adhesion bonding. To overcome the hydration repulsive forces, for instance mussel apply forces and/or dry the surface using Mfps [12]. In the literature, surface force apparatus (SFA) and atomic force microscope (AFM) have been commonly used to determine the adhesion with applying forces [4,13]. On the other hand, achieving adhesion without applying force might be more valuable especially for clinical treatments. Spectroscopic techniques e.g. X-ray photoelectron spectroscopy (XPS), Raman spectroscopy, infrared spectroscopy and dynamic nuclear polarization (DNP) have been used to monitor adhesion without applying external force [14–17]. In addition to them, we used as a first time electron paramagnetic resonance (EPR) spectroscopy in our previous studies to determine the spontaneous wet adhesion of Mfps and DOPA functionalized poly(ethylene glycol) polymer (PEG) to spin labeled polystyrene and silica nanoparticles [5,6,17].

EPR spectroscopy in combination with spin labeling has been increasingly used in protein, polymer and drug delivery studies [18–21]. In aqueous solutions, dynamics behaviors of spin labels characterized with rotational correlation times affect the EPR line shapes. Therefore, spin labels that have free or restricted motions yield sharp (corresponding to fast rotational correlation time) or broad (corresponding to slow rotational correlation time) EPR lines, respectively [18]. This provides observations of different types of spin labels simultaneously.

Using EPR spectroscopy, spin labels on polystyrene or silica nanosurfaces report surface coverage upon addition of adhesive materials since second type of signal (broader signal) is observed upon adhesion. The areas under EPR signals of covered and uncovered spin labels gives the percentage of surface coverage. For example, addition of 180 mg/mL of DOPA functionalized four armed PEG polymer (PEG-$(DOPA)_4$) to the spin labeled polystyrene nanoparticle results in an 82% of surface coverage [5]. However, neither of Mfps and DOPA containing PEG polymers attached to the silica surface performed under the same conditions.

For the spontaneous DOPA wet-adhesion, the hydration repulsion force becomes one of the determining factors. Hydration layers around both the hydrophilic silica nanoparticles and DOPA containing Mfps and PEG polymers form barriers between them. On the other hand, weakening hydration layers of silica may help DOPA adhesion. For example, adsorption of surfactant molecules to the silica surface may disturb the hydration shells of silica. Alkyl side of surfactant molecule could interfere the distribution of hydration water molecules. Also, interaction between DOPA and silica surface could be possible during cross-linking of DOPA functionalized PEG polymers in the presence of oxidizing agents. Depends on the gelation mechanism, DOPA could penetrate the hydration barriers and interact with silica surface. Fast hardening of DOPA containing polymers can be considered as an applied force to break the hydration barriers of silica surface.

Here, we aim to compare the wet adhesive properties of DOPA modified four armed poly(ethylene glycol) polymer (PEG-$(DOPA)_4$) and its hydrogels induced by $(IO_4)^-$ and $(Cr_2O_7)^{2-}$ ions by using EPR spectroscopy. Without applying external force, DOPA containing polymer and hydrogels adhere to hydrophobic polystyrene and hydrophilic silica surfaces differently. This method allows us to compare the adhesive materials in terms of their ability to cover the surface of colloidal nanoparticles.

2. Experimental procedure

The synthesis of PEG-$(DOPA)_4$ was prepared as described in published procedures [5,22,23].

2.1. Synthesis of protected DOPA

L-DOPA (78.85 mg, 0.4 mmol) and triethylamine (86 μL) were mixed in water:dioxane (1:1) mixture (800 μL) in an ice bath (0 °C). The mixture was stirred at 0 °C until all compounds were dissolved. Afterwards, di-tert-butyl dicarbonate (98 mg, 0.45 mmol) was dissolved in dioxane (400 μL) and added into the mixture containing L-DOPA and triethylamine, and stirred at 0 °C for 30 min. After 30 min, the mixture was stirred at 25 °C for 17 h. At the end of the reaction, the mixture was extracted with ethyl acetate (50 mL) and the pH of the organic phase was adjusted to 1.0 by HCl and back extracted with ethyl acetate (50 mL) for 3 times. Combined organic phases were dried over Na_2SO_4. Organic solvent was evaporated to afford N-Boc-L-DOPA as a brown oil which was used in the next step without any purification (100.4 mg, 80% yield). ^{1}H NMR (400 MHz, DMSO-d_6) δ: 6.87 (d, 1H), 6.58 (d, 2H), 6.44 (d, 1H), 4.01–3.93 (m, 1H), 2.79–2.58 (m, 2H), 1.30 (s, 9H).

2.2. Synthesis of PEG-$(DOPA)_4$

PEG-$(NH_2)_4$ (10,000 g/mol) (97 mg, 9.7×10^{-3} mmol), protected-DOPA (23.9 mg, 80 mmol), 1-hydroxybenzotriazol (HOBT) (17.3 mg, 0.128 mmol) and triethylamine (17.6 μL) were mixed in a mixture of DCM (460 μL) and DMF (460 μL) at 25 °C until all compounds were dissolved. 2-(1H-benzotriazol-1-yl)-1,1,3,3-tetramethyluronium hexafluorophosphate (HBTU) (29.6 mg, 0.078 mmol) and DCM (460 μL) were added into the mixture and stirred at 25 °C under argon atmosphere for 5 h. At the end of the experiment ninhydrine test was applied to control if there is any primary amine in the experiment medium. 2–3 drops of product were dissolved in DCM (1 mL) and 2–3 drops of ninhydrine solution was put into the solution. The mixture was stirred at 50 °C for 30 min, the test result was negative.

The crude product was washed with saturated sodium chloride solution (50 mL), $NaHCO_3$ (5% w/mL) solution, HCl (1 M) solution (50 mL), and distilled water (50 mL). The organic phase was dried over Na_2SO_4 and the product was precipitated in cold diethyl ether for 3 times to afford PEG-(N-Boc-L-$DOPA)_4$ as white solid (75.5 mg, 70% yield). ^{1}H NMR (400 MHz, $CDCl_3$) δ: 6.77 (t, 8H), 6.57 (d, 4H), 6.15 (s, 4H), 4.21 (s, 4H), 3.81 (t, 8H), 3.64–3.45 (m, 896H), 3.00 (d, 8H), 2.72 (t, 8H), 1.41 (s, 36H). In this study, the attached DOPA groups to PEG are all N-Boc protected.

2.3. Hydrogel preparation

Final concentrations of 0.12 mM PEG-$(DOPA)_4$ and cross-linkers sodium (meta) periodate, $NaIO_4$, or bis(tetrabutylammonium) dichromate, $[(CH_3CH_2CH_2CH_2)_4N]_2Cr_2O_7$, were dissolved in 0.2 M MES buffer at pH 3.0. The ratio of DOPA:cross-linkers are 1:3 and 1:1, respectively. After mixing, solutions colours were changed in a few minutes from transparent to yellow and orange for $(IO_4)^-$ and $(Cr_2O_7)^{2-}$ cross-linkers, respectively and analysed with UV–vis spectroscopy.

For the EPR measurements PEG-$(DOPA)_4$ in MES buffer at pH 3.0 was mixed with $(IO_4)^-$ or $(Cr_2O_7)^{2-}$ oxidizing agents. Then, the obtained hydrogel fluids were transferred immediately to the spin labeled nanoparticle solution (1:1 (v:v) ratio) prepared in MES buffer at pH 3.0 with a micropipette (Fig. 1). Final concentration of PEG-$(DOPA)_4$ was adjusted to 45 mg/mL. Acidic medium was used to avoid DOPA oxidation.

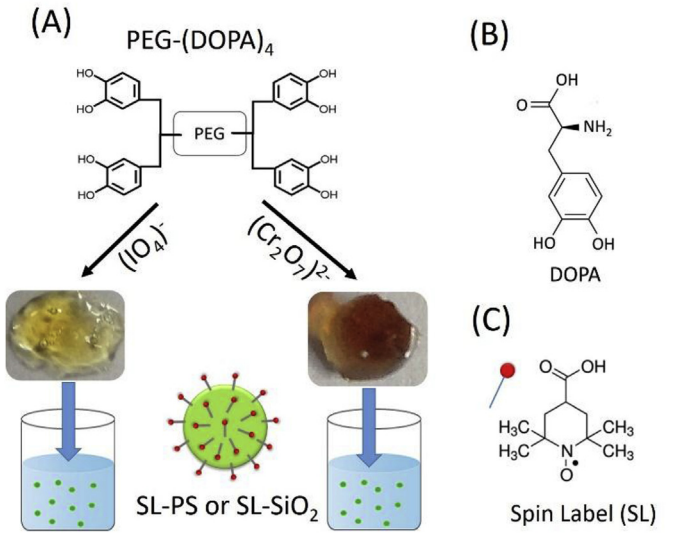

Fig. 1. Schematic representations of (A) PEG-$(DOPA)_4$ hydrogel formation with $(IO_4)^-$ and $(Cr_2O_7)^{2-}$ ions, and their mixtures with SL-PS or SL-SiO_2 nanoparticles in MES buffer at pH 3.0, (B) DOPA and (C) 4-carboxy Tempo as spin label (SL).

2.4. Preparation of SL-nanoparticles

A nitroxide type 2,2,6,6-tetramethylpiperidine-1-oxyl (Tempo) based spin label was used. 250 µL 4-carboxy Tempo (10 mM) dissolved in 0.2 M MES buffer (pH 3.0) was mixed with 100 µL amine-modified polystyrene bead (Sigma Aldrich, 50 nm particle size) or 100 µL 3-aminopropyl functionalized silica (Sigma Aldrich, < 100 nm particle size), in the presence of a cross linker, 38 mM, 90 µL 1-ethyl-3-(3-dimethylaminopropyl) carbodiimide (EDC) (Thermo Scientific) for one day at room temperature [17]. Excess EDC and 4-carboxy Tempo were washed out several times with MES buffer at pH 3.0. A Malvern dynamic light scattering (DLS) Nano-ZS instrument (Worcestershire, UK) was used for size and zeta potential measurements of nanoparticles. The nanoparticles were diluted 1: 100 with MES buffer prior to measurement and measured at 25 °C at a scattering angle of 90°. The zeta potential was measured by a zeta potential analyzer using electrophoretic laser Doppler anemometry. The measured SL-PS and SL-SiO_2 beads diameters are about 50 nm with PDI values less than 0.2.

2.5. EPR measurements and calculations of surface coverage

X-band EPR measurements were done using a CMS 8400 (Adani) benchtop spectrometer at room temperature in the quartz capillary tubes. EPR spectra were simulated using a matlab based Easyspin 4.5.5 software package [24].

EPR spectra of SL-PS and SL-SiO_2 after addition of PEG-$(DOPA)_4$ polymer or hydrogels were simulated using individual spectral simulations of covered (A) and uncovered (B) spin labels. The complete simulations of experimental results were obtained by combining the individual components, (A) and (B) with appropriate numbers as given by:

$$\text{Measured spectrum} = x_{(A)}sim_{(A)} + x_{(B)}sim_{(B)} \quad (1)$$

Where the simulated individual spectra of A ($sim_{(A)}$) and B ($sim_{(B)}$) are multiplied by the appropriate numbers, $x_{(A)}$ and $x_{(B)}$.

The surface coverage percentage is calculated by the areas under each spectrum ($sim_{(A)}$ and $sim_{(B)}$) found by double integration, and multiplied by the numbers $x_{(A)}$ and $x_{(B)}$, as given by:

$$\%\text{Covering} = \text{Covered Area} / (\text{Covered Area} + \text{Uncovered Area}) \quad (2)$$

Where covered area is calculated from the multiplication of area under $sim_{(A)}$ with $x_{(A)}$, and uncovered area is calculated from the multiplication of area under $sim_{(B)}$ with $x_{(B)}$.

3. Results and discussion

3.1. Characterization of PEG-$(DOPA)_4$ and hydrogels with UV–vis spectroscopy

UV–vis absorption spectra of 0. 12 mM PEG-$(NH_2)_4$ and synthesized PEG-$(DOPA)_4$ were compared to show DOPA conjugation in MES buffer at pH 3.0 (Fig. 2). For the UV–vis spectrum of PEG-$(DOPA)_4$, the absorption signal at 278 nm corresponds to the catechol moiety which confirms the presence of the reduced form of DOPA [25]. As expected, PEG-$(NH_2)_4$ does not have an absorption signal. Hydrogel formation of PEG-$(DOPA)_4$ with $(IO_4)^-$ and $(Cr_2O_7)^{2-}$ were also followed by UV–vis spectroscopy (Fig. 2). Concentrations of $(IO_4)^-$ and $(Cr_2O_7)^{2-}$ are 1.44 mM and 0.48 mM, and the ratios of DOPA:cross-linker are 1:3 and 1:1, respectively. After addition of the $(IO_4)^-$, a new broad signal at 395 nm and a shoulder at 325 nm were observed, corresponding to DOPA quinone and α,β-dehydrodopamine, respectively [26]. While DOPA quinone signal decreased, α,β-dehydrodopamine signal increased with time, leading to subsequent polymerization. In addition, catechol groups transformed into phenolic intermediates with similar absorbance values. Therefore, the signal around 278 nm increased continuously. On the other hand, the UV–vis spectrum of hydrogel induced by the $(Cr_2O_7)^{2-}$ yielded the characteristic signal of $(Cr_2O_7)^{2-}$ ion at 348 nm [27]. In addition, broad signals around 278 nm and 450 nm were appeared immediately. With time, the signal at 348 nm gradually decreased due to the reduction of Cr(VI) and broad signals around 278 nm and 450 nm increased due to the polymerization of DOPA at pH

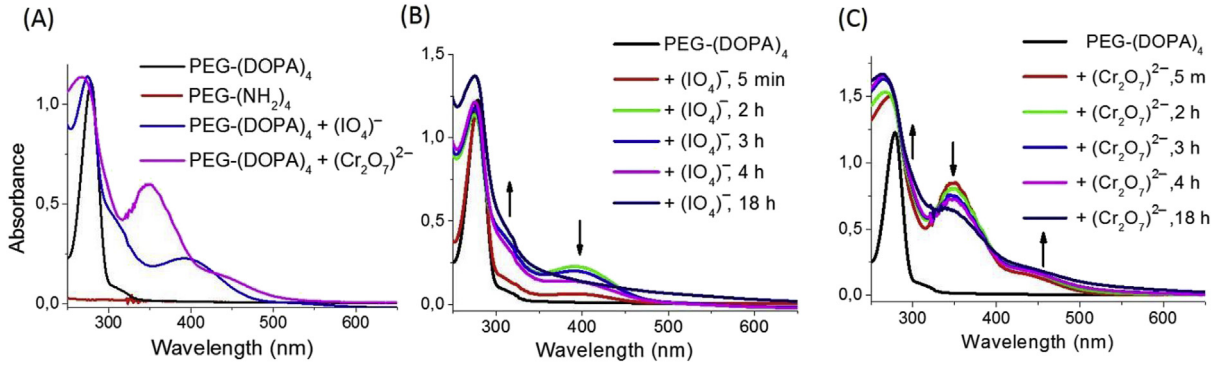

Fig. 2. (A) UV–vis spectra of PEG-$(NH_2)_4$, PEG-$(DOPA)_4$, PEG-$(DOPA)_4$ + $(IO_4)^-$ hydrogel and PEG-$(DOPA)_4$ + $(Cr_2O_7)^{2-}$ hydrogel. Time dependent UV–vis absorption results of PEG-$(DOPA)_4$ + $(IO_4)^-$ hydrogel (B) and PEG-$(DOPA)_4$ + $(Cr_2O_7)^{2-}$ hydrogel (C). Concentrations of PEG polymers and cross-linkers ($(IO_4)^-$ and $(Cr_2O_7)^{2-}$) are 0.12 mM, 1.44 mM, and 0.48 mM, respectively. The attached DOPA groups to PEG are all N-Boc protected.

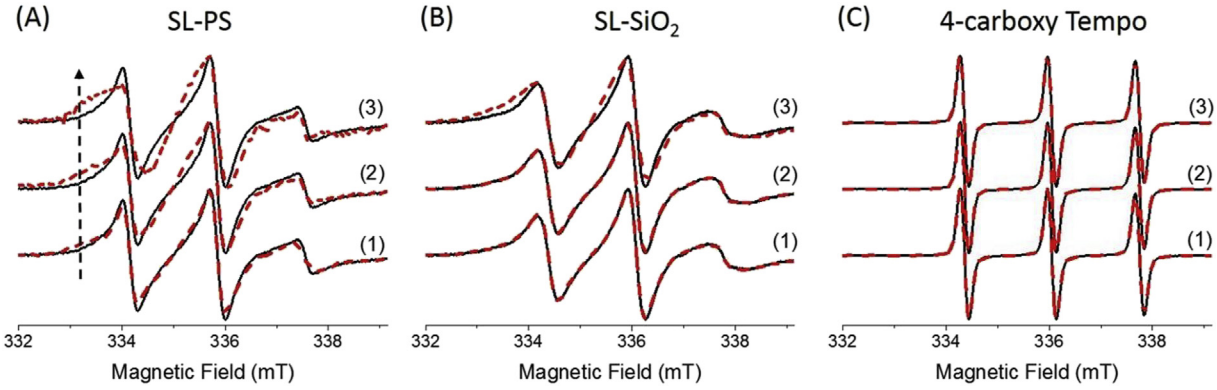

Fig. 3. EPR spectra of SL-PS (A), SL-SiO_2 (B), and 4-carboxy Tempo (C), black solid lines, and after additions of 45 mg/mL of PEG-$(DOPA)_4$ (1), $(IO_4)^-$ induced PEG-$(DOPA)_4$ hydrogel (2), and $(Cr_2O_7)^{2-}$ induced PEG-$(DOPA)_4$ hydrogel (3), red dashed lines. The ratio of DOPA:cross-linker is 1:3 and 1:1 for $(IO_4)^-$ and $(Cr_2O_7)^{2-}$, respectively. The attached DOPA groups to PEG are all N-Boc protected. (For interpretation of the references to colour in this figure legend, the reader is referred to the Web version of this article.)

3.0.

3.2. Determination of surface adhesion using EPR spectroscopy

EPR spectroscopy can be used in systems having paramagnetic molecules. Although, most of the systems are diamagnetic, they can be still studied with EPR spectroscopy associated with spin labeling method. Here, Tempo based stable nitroxide radicals are used as spin labels. 4-carboxy Tempo has been covalently attached to amine sides of polystyrene or silica surfaces by carbodiimide chemistry.

In solution, EPR line shape analysis allows monitoring the changes on the surface of nanoparticles [5,17]. Spin labels on the surface of nanoparticles behaves like reporters for the possible adhesive interactions. Spin labels buried under the adhesive molecules could lose their motion flexibility, and thus rotational correlation time (τ_R) of the spin label increases. EPR spectra of the bare SL-PS (τ_R = 2.8 ns) and SL-SiO_2 (τ_R = 2.9 ns) nanoparticles are shown in Fig. 3A and B (black lines), respectively. Their τ_R numbers found by simulations showed that spin label attached on the nanoparticles has nearly a hundred times slower motions compared to the motion of free spin label (4-carboxy Tempo) in the solution, τ_R = 20 ps (Fig. 3C). Also, addition of 45 mg/mL of PEG-$(DOPA)_4$ to the SL-PS solution further slows down the motions of some spin labels on PS from 2.8 ns to 10 ns. Since DOPA groups attach to the PS surface via hydrophobic interactions, they cover the spin labels and restricts the motion of them [17]. In the previous studies, using EPR spectroscopy, we showed that Mfps and PEG-$(DOPA)_4$ can adhere to polystyrene without applying force in the solution but PEG-$(NH_2)_4$ cannot adhere to polystyrene [5,6,17]. This shows the function of DOPA in the wet adhesion. Also, these results showed that the PEG polymer without DOPA groups does not have a wet adhesion ability.

EPR spectroscopy can be also used to study the adhesive properties of hydrogels. PEG-$(DOPA)_4$ polymers can be transformed into hydrogels with the help of oxidizing agents [23]. Here, $(IO_4)^-$ and $(Cr_2O_7)^{2-}$ were used to cross-link the DOPA molecules and to obtain cured adhesive materials at pH 3.0. Similar to the result of PEG-$(DOPA)_4$ addition, EPR spectrum of SL-PS changed after additions of both types of hydrogels (Fig. 3A, (2) and (3), red). Hydrogels were added into nanoparticle solution while they were still fluids. Simulations of their EPR spectra revealed that two types of signals with different τ_R values were obtained (Fig. 4A). The shorter τ_R value with 2.8 ns belongs to uncovered spin labels on polystyrene, and the longer τ_R values with 8 ns and 9 ns belong to spin labels on polystyrene that are covered by $(Cr_2O_7)^{2-}$ and $(IO_4)^-$ induced hydrogels, respectively.

Adhesion behaviors of PEG-$(DOPA)_4$ polymers and hydrogels on the hydrophilic surface of silica nanoparticles are also different (Fig. 3B). It has been known that DOPA can adhere to the wet silica surface upon applied force [28], however strong hydration layers around the silica form barriers between DOPA and silica surface which averts the spontaneous adhesion [5,17]. Therefore, the EPR spectrum of bare SL-SiO_2 did not change upon addition of 45 mg/mL of PEG-$(DOPA)_4$ (Fig. 3B (1) red). Similarly, cross-linked PEG-$(DOPA)_4$ hydrogels prepared with the $(IO_4)^-$ did not adhere to the surface of silica nanoparticles (Fig. 3B (2) red). Instead, hydrogel of PEG-$(DOPA)_4$ cross-linked with the help of $(Cr_2O_7)^{2-}$ adhered to the silica nanoparticles in solution (Fig. 3B (3) red). Two types of EPR signals, covered (τ_R = 8 ns) and uncovered (τ_R = 2.9 ns) types, were observed upon addition of hydrogel (Fig. 4B).

In addition, the percentages of covered spin labels on the nanoparticles can be calculated from the double integrations of the simulated EPR spectra of covered and uncovered spin labels (Fig. 5). According to simulations and calculations explained in the experimental part, we observed that 65%, 76% and 93% of the spin labels on the polystyrene were covered upon additions of PEG-$(DOPA)_4$ polymer, $(IO_4)^-$ induced PEG-$(DOPA)_4$ hydrogel and $(Cr_2O_7)^{2-}$ induced PEG-$(DOPA)_4$ hydrogel, respectively (Fig. 6). These findings showed that DOPA hydrogels compared to the PEG-$(DOPA)_4$ polymer adhere to the polystyrene surface more extensively. Moreover, according to simulations of spin labels on silica nanoparticles after $(Cr_2O_7)^{2-}$ induced PEG-$(DOPA)_4$ hydrogel adhesion, 59% of spin labels on silica were covered (Fig. 6).

The effect of viscosity increasing on the spin label dynamics was studied with free spin label of 4-carboxy Tempo. Rotational correlation time of a spin label increases in a viscous solution due to the restriction of motion [29]. However, EPR spectrum of free spin label in solution did not change upon additions of hydrogels (Fig. 3C). This can be explained by the dissolution of spin labels in the water pools of hydrogels. Therefore, dynamics of spin labels are not affected from the bulk viscosity of the hydrogels.

A similar trend in the adhesive functions of poly[(3,4-dihydroxystyrene)-*co*-styrene] and PEG-$(DOPA)_4$ was observed after cured with $(IO_4)^-$ and $(Cr_2O_7)^{2-}$ [7]. It has been known that $(IO_4)^-$ initiates covalent cross-linking of PEG-$(DOPA)_4$ molecules [23]. Instead, coordinated cross-linked PEG-$(DOPA)_4$ hydrogel was obtained with $(Cr_2O_7)^{2-}$. At pH 3.0, $(Cr_2O_7)^{2-}$ induced PEG-$(DOPA)_4$ hydrogel was completely dissolved overnight in the EDTA solution which is a chelating agent. However, $(IO_4)^-$ induced gel did not dissolve in the EDTA solution due to the formation of covalent cross-linked DOPA molecules (Fig. 7). In the literature, $(Cr_2O_7)^{2-}$ ion was proved to be the strongest inducer of hardening for Mfps and also for the poly[(3,4-dihydroxystyrene)-*co*-styrene] polymers [7,9]. Also, its curing mechanism is faster than that of $(IO_4)^-$ ion at pH 3.0. For the spontaneous adhesion, hardening of hydrogel in a few minutes could be considered as an applied force to break the hydration layers of SiO_2 surface. These could be the reasons for the better

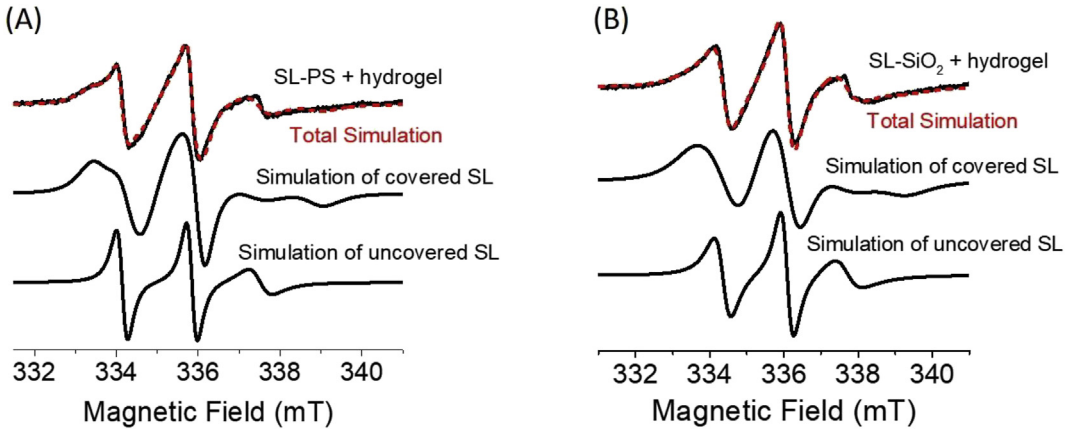

Fig. 4. (A) EPR spectrum of SL-PS after addition of $(IO_4)^-$ induced PEG-$(DOPA)_4$ hydrogel (black) and its simulation (red). (B) EPR spectrum of SL-SiO_2 after addition of $(Cr_2O_7)^{2-}$ induced PEG-$(DOPA)_4$ hydrogel (black) and its simulation (red). The simulated spectrum was obtained by the addition of simulated covered SL and uncovered SL. (For interpretation of the references to colour in this figure legend, the reader is referred to the Web version of this article.)

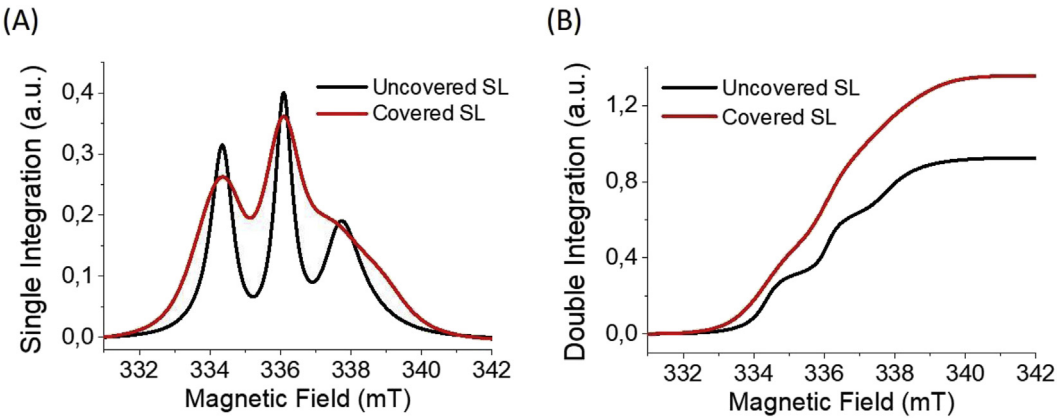

Fig. 5. (A) Single integrations of simulated spectra of covered and uncovered spin labels (SL) on SiO_2 nanoparticles upon addition of 45 mg/mL of PEG-$(DOPA)_4$ hydrogel induced by $(Cr_2O_7)^{2-}$ ions. (B) Double integrations of spectra in (A). Double integration gives the area under the EPR spectrum.

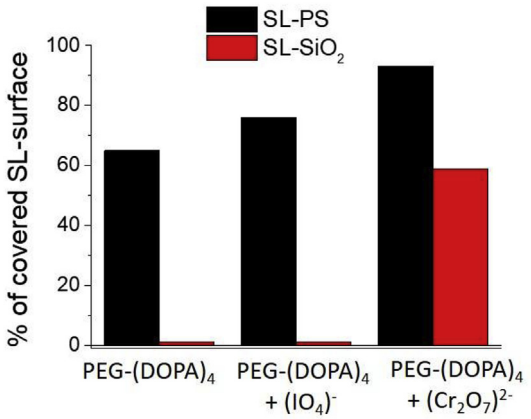

Fig. 6. The percentages of covered spin labels on SL-PS (black) and SL-SiO_2 (red) after additions of PEG-$(DOPA)_4$ polymer, $(IO_4)^-$ induced PEG-$(DOPA)_4$ hydrogel and $(Cr_2O_7)^{2-}$ induced PEG-$(DOPA)_4$ hydrogel. (For interpretation of the references to colour in this figure legend, the reader is referred to the Web version of this article.)

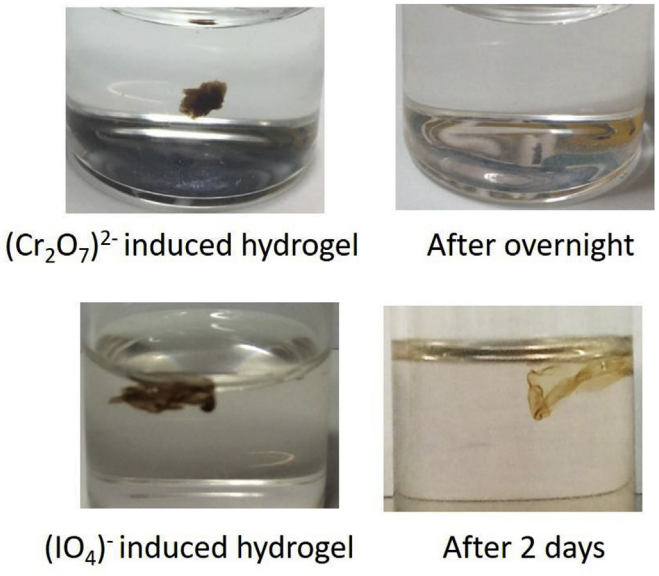

Fig. 7. 10 times excess EDTA relative to concentrations of $(Cr_2O_7)^{2-}$ and $(IO_4)^-$ ions were added to the hydrogel samples.

adhesion ability of $(Cr_2O_7)^{2-}$ induced PEG-$(DOPA)_4$ hydrogel to the both polystyrene and silica nanoparticles.

In order to improve the surface coverage with spontaneous adhesion, the concentration PEG-$(DOPA)_4$ was increased in the solutions of spin labeled polystyrene or silica nanoparticles and studied with EPR spectroscopy [5]. As the final concentrations of PEG-$(DOPA)_4$ increases from 11 mg/mL to 180 mg/mL, the surface coverage of polystyrene increases from 49% to 82%. However, PEG-$(DOPA)_4$ did not adhere to silica surface even at 180 mg/mL of concentration. On the other hand,

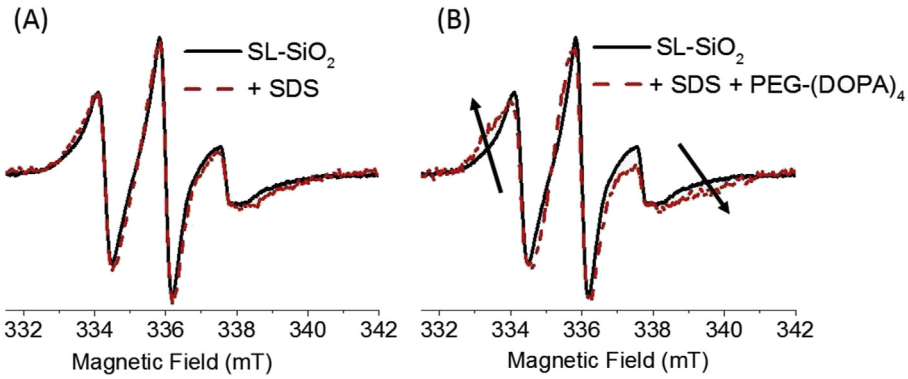

Fig. 8. (A) EPR spectra of SL-SiO_2 before (black) and after addition of SDS (2 mM) (red). (B) EPR spectra of SL-SiO_2 before (black) and after addition of SDS (2 mM) and PEG-$(DOPA)_4$ (40 mg/mL) (red). The attached DOPA groups to PEG are all N-Boc protected. (For interpretation of the references to colour in this figure legend, the reader is referred to the Web version of this article.)

hydrogel forms of PEG-$(DOPA)_4$ adhere to both polystyrene and silica surfaces much better than the PEG-$(DOPA)_4$ polymer at the same concentrations. For the $(Cr_2O_7)^{2-}$ induced hydrogel prepared even with 45 mg/mL of PEG-$(DOPA)_4$ concentration, 93% and 59% of the surface coverages for polystyrene and silica nanoparticles were obtained.

Another way to succeed spontaneous wet adhesion of DOPA on hydrophilic silica surface is weakening hydration shells of the surface. Since hydration layers obstruct the spontaneous adhesion, they could be distracted upon additions of different solvents or attachment of hydrophobic molecules on surface. When less polar water-miscible solvent of dioxane was mixed with MES buffer containing silica nanoparticles, it did not promote the spontaneous adhesion. EPR spectra of spin labeled silica in MES buffer:dioxane (1:6, v:v) mixture before and after addition of PEG-$(DOPA)_4$ were almost identical. This shows that dioxane could not displace the hydration water molecules on silica.

Next, an anionic surfactant molecule of sodium dodecyl sulfate (SDS) was used to disturb the hydration layers of silica. Since silica surface is functionalized with amine groups, the nanoparticles are cationic at pH 3.0. In addition, after spin labeling silica nanoparticles are still positively charged with a zeta potential of +14 mV. Addition of SDS solution with a final concentration of 2 mM neutralizes the nanoparticles in charge, with a zeta potential of approximately 0 mV. While anionic part of SDS attaches to the positively charged silica surface, hydrophobic part of SDS become accessible to hydration water molecules. Fig. 8A shows the EPR spectra of SL-SiO_2 before and after addition of SDS (2 mM). Adsorption of SDS molecules on silica nanoparticles does not change the EPR spectrum of SL-SiO_2 significantly. On the other hand, the EPR line shape of SL-SiO_2 has changed and a second type of signal was observed upon addition of PEG-$(DOPA)_4$ polymer (45 mg/mL) on the SDS adsorbed SL-SiO_2 nanoparticles (Fig. 8B). This shows that PEG-$(DOPA)_4$ is able to adhere to wet silica surface after the strong hydration barriers of silica are disturbed with the presence of SDS.

4. Conclusion

EPR spectroscopy can be used as a direct method for the determination of surface coverage upon addition of adhesive materials. Spin labels attached on the surface allow monitoring the adhesion. Since the EPR spectra of covered and uncovered spin labels are different, they can be differentiated in the same spectrum. The ratio of covered and uncovered signals are used to calculate the fraction of surface coverage.

Here, without applying an external force, we determined the significant adhesion ability of $(Cr_2O_7)^{2-}$ induced PEG-$(DOPA)_4$ hydrogels to the both SL-PS and SL-SiO_2 nanoparticles in solution with EPR spectroscopy. About 93% of spin labels on polystyrene and 59% of spin labels on SiO_2 are covered with the PEG-$(DOPA)_4$ hydrogel cured with $(Cr_2O_7)^{2-}$. Although, PEG-$(DOPA)_4$ polymer and hydrogel induced with $(IO_4)^-$ ions adhere to polystyrene with surface coverages 65% and 76%, respectively, they cannot adhere to SiO_2 surface due to the strong hydration layers around the silica.

Gelation mechanisms of PEG-$(DOPA)_4$ polymers depend on the types of cross-linkers. Using $(Cr_2O_7)^{2-}$ ions, coordinated type of cross-linking results in a fast and high degree hardening that helps DOPA to penetrate the hydration layers of both polystyrene and silica surface. On the other hand, covalently cross-linked PEG-$(DOPA)_4$ hydrogel cannot penetrate the strong hydration barriers of silica. This shows the importance of gelation mechanism of DOPA for the spontaneous wet adhesion. Another way to achieve spontaneous wet adhesion to silica surface is weakening the strong hydration layers. Adsorption of SDS surfactant molecules on silica disturbs the hydration layers and PEG-$(DOPA)_4$ could adhere to silica spontaneously.

Acknowledgements

This work was supported by Turkish Scientific and Technological Research Council (Tubitak) via 3501 Program under grant 114Z318.

References

[1] P.B. Lee, P.B. Messersmith, J.N. Israelachvili, H. Waite, Mussel-inspired adhesives and coatings, Annu. Rev. Mater. Res. 41 (2011) 99–132.
[2] J.H. Waite, X.X. Qin, Polyphosphoprotein from the adhesive pads of Mytilus edulis, Biochemistry 40 (2001) 2887–2893.
[3] J. Yang, M.A.C. Stuart, M. Kamperman, Jack of all trades: versatile catechol crosslinking mechanisms, Chem. Soc. Rev. 43 (2014) 8271–8298.
[4] H. Lee, N.F. Scherer, P.B. Messersmith, Single-molecule mechanics of musse adhesion, Proc. Natl. Acad. Sci. U.S.A. 103 (2006) 12999–13003.
[5] İ. Kırpat, Y. Göksel, E. Karakuş, M. Emrullahoğlu, Y. Akdogan, Determination of force-free wet adhesion of mussel-inspired polymers to spin labeled surface, Mater. Lett. 205 (2017) 48–51.
[6] Y. Göksel, İ. Kırpat, Y. Akdogan, Spontaneous adhesion of DOPA and tryptophan functionalized PEG to polystyrene nanobeads: an EPR study, Mater. Sci. Forum 915 (2018) 243–247.
[7] G. Westwood, T.N. Horton, J.J. Wilker, Simplified polymer mimics of cross-linking adhesive proteins, Macromolecules 40 (2007) 3960–3964.
[8] A. Doraiswamy, T.M. Dunaway, J.J. Wilker, R.J. Narayan, Designing biomaterials for 3D printing, J. Biomed. Mater. Res. B: Appl. Mater. 89B (2009) 28–35.
[9] J. Monahan, J.J. Wilker, Cross-linking the protein precursor of marine mussel Adhesives: bulk measurements and reagents for curing, Langmuir 20 (2004) 3724–3729.
[10] H. Xu, J. Nishida, W. Ma, H. Wu, M. Kobayashi, H. Otsuka, A. Takahara, Competition between oxidation and coordination in cross-linking of polystyrene copolymer containing catechol groups, ACS Macro Lett. 1 (2012) 457–460.
[11] D.G. Barrett, D.E. Fullenkamp, L. He, N. Holten-Andersen, K. Yee, C. Lee, P.B. Messersmith, pH-based regulation of hydrogel mechanical properties through mussel-inspired chemistry and processing, Adv. Funct. Mater. 23 (2013) 1111–1119.
[12] N.R.M. Rodriguez, S. Das, Y. Kaufman, J.N. Israelachvili, J.H. Waite, Interfacial pH during mussel adhesive plaque formation, Biofouling 31 (2015) 221–227.
[13] J. Yu, Y. Kan, M. Rapp, E. Danner, W. Wei, S. Das, D.R. Miller, Y. Chen, J.H. Waite, J.N. Israelachvili, Adaptive hydrophobic and hydrophilic interactions of mussel foot proteins with organic thin films, Proc. Natl. Acad. Sci. U.S.A. 110 (2013) 15680–15685.
[14] Y. Kan, E.W. Danner, J.N. Israelachvili, Y. Chen, J.H. Waite, Boronate complex formation with Dopa containing mussel adhesive protein retards ph-induced oxidation and enables adhesion to mica, PLoS One 9 (2014) e108869.
[15] A.A. Ooka, R.L. Garrell, Surface-enhanced Raman spectroscopy of DOPA-containing peptides related to adhesive protein of marine mussel, Mytilus edulis. *Biopolymers (Biospectroscopy)* 57 (2000) 92–102.
[16] W. Wei, L. Petrone, Y. Tan, H. Cai, J.N. Israelachvili, A. Miserez, J.H. Waite, An

underwater surface-drying peptide inspired by a mussel adhesive protein, Adv. Funct. Mater. 26 (2016) 3496–3507.
[17] Y. Akdogan, W. Wei, K.Y. Huang, Y. Kageyama, E.W. Danner, D.R. Miller, N.R.M. Rodriguez, J.H. Waite, S. Han, Intrinsic surface-drying properties of bioadhesive proteins, Angew. Chem. Int. Ed. 53 (2014) 11253–11256.
[18] C. Altenbach, C.J. Lopez, K. Hideg, W.L. Hubbell, Exploring structure, dynamics, and topology of nitroxide spin-labeled proteins using continuous-wave electron paramagnetic resonance spectroscopy, Methods Enzymol. 564 (2015) 59–100.
[19] U. Lappan, B. Wiesner, U. Scheler, Segmental dynamics of poly(acrylic acid) in polyelectrolyte complex coacervates studied by spin-label EPR spectroscopy, Macromolecules 49 (2016) 8616–8621.
[20] Y. Akdogan, M. Emrullahoğlu, D. Tatlidil, M. Ucuncu, G. Cakan-Akdogan, EPR studies of intermolecular interactions and competitive binding of drugs in a drug–BSA binding model, Phys. Chem. Chem. Phys. 18 (2016) 22531–22539.
[21] D. Tatlidil, M. Ucuncu, Y. Akdogan, Physiological concentrations of albumin favour drug binding, Phys. Chem. Chem. Phys. 17 (2015) 22678–22685.
[22] G. Giorgioni, F. Claudi, S. Ruggieri, M. Ricciutelli, G.F. Palmieri, A. Di Stefano, P. Sozio, L.S. Cerasa, A. Chiavaroli, C. Ferrante, G. Orlando, R.A. Glennon, Design, synthesis, and preliminary pharmacological evaluation of new imidazolinones as L-DOPA prodrugs, Bioorg. Med. Chem. 18 (2010) 1834–1843.
[23] B.P. Lee, J.L. Dalsin, P.B. Messersmith, Synthesis and gelation of DOPA-modified poly(ethylene glycol) hydrogels, Biomacromolecules 3 (2002) 1038–1047.
[24] S. Stoll, A. Schweiger, EasySpin, a comprehensive software package for spectral simulation and analysis in EPR, J. Magn. Reson. 178 (2006) 42–55.
[25] L.M. Rzepecki, T. Nagafuchi, J.H. Waite, alpha,beta-Dehydro-3,4- dihydroxyphenylalanine derivatives: potential schlerotization intermediates in natural composite materials, Arch. Biochem. Biophys. 285 (1991) 17–26.
[26] M. Cencer, Y. Liu, A. Winter, M. Murley, H. Meng, B.P. Lee, Effect of pH on the rate of curing and bioadhesive properties of dopamine functionalized poly(ethylene glycol) hydrogels, Biomacromolecules 15 (2014) 2861–2869.
[27] J.B. Borah, H. Saikia, P. Bharali, Reductive conversion of Cr(VI) to Cr(III) over bimetallic CuNi nanocrystals at room temperature, New J. Chem. 38 (2014) 2748–2751.
[28] Q. Lu, E. Danner, J.H. Waite, J.N. Israelachvili, H. Zeng, D.S. Hwang, Adhesion of mussel foot proteins to different substrate surfaces, J. R. Soc. Interface 10 (2013) 20120759.
[29] J.S. Hwang, R.P. Mason, L.P. Hwang, J.H. Freed, Electron spin resonance studies of anisotropic rotational reorientation and slow tumbling in liquid and frozen media. III. Perdeuterated 2,2,6,6-tetramethyl-4-piperidone N-oxide and an analysis of fluctuating torques, J. Phys. Chem. 79 (1975) 489–511.